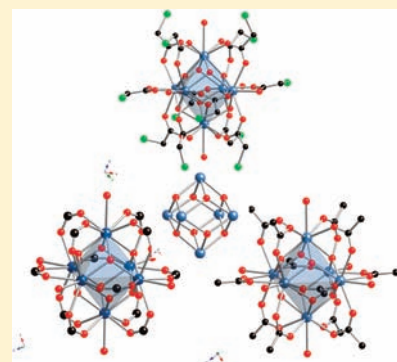


Thorium(IV) Molecular Clusters with a Hexanuclear Th Core

Karah E. Knope,[†] Richard E. Wilson,[†] Monica Vasiliu,[‡] David A. Dixon,^{†,‡} and L. Soderholm^{*,†}[†]Chemical Sciences and Engineering Division, Argonne National Laboratory, Argonne, Illinois 60439, United States[‡]Chemistry Department, The University of Alabama, Shelby Hall, Box 870336, Tuscaloosa, Alabama 35487-0336, United States

Supporting Information

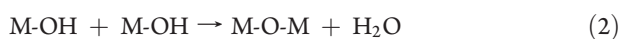
ABSTRACT: Three polynuclear thorium(IV) molecular complexes have been synthesized under ambient conditions from reactions of an amorphous Th precipitate, obtained via hydrolysis, with carboxylate functionalized ligands. The structures of $\text{Th}_6(\text{OH})_4\text{O}_4(\text{H}_2\text{O})_6(\text{HCO}_2)_{12} \cdot n\text{H}_2\text{O}$ (1), $\text{Th}_6(\text{OH})_4\text{O}_4(\text{H}_2\text{O})_6(\text{CH}_3\text{CO}_2)_{12} \cdot n\text{H}_2\text{O}$ (2), $\text{Th}_6(\text{OH})_4\text{O}_4(\text{H}_2\text{O})_6(\text{ClCH}_2\text{CO}_2)_{12} \cdot 4\text{H}_2\text{O}$ (3) each consist of a hexanuclear Th core wherein six 9-coordinate Th(IV) cations are bridged by four μ_3 -hydroxo and four μ_3 -oxo groups. Each Th(IV) center is additionally coordinated to one bound “apical” water molecule and four oxygen atoms from bridging carboxylate functionalized organic acid units. “Decoration” of the cationic $[\text{Th}_6(\mu_3\text{-O})_4(\mu_3\text{-OH})_4]^{12+}$ cores by anionic shells of R-COO[−] ligands (R = H, CH₃, or CH₂Cl) terminates the oligomers and results in the formation of discrete, neutral molecular clusters. Electronic structure calculations at the density functional theory level predicted that the most energetically favorable positions for the protons on the hexanuclear core result in the cluster with the highest symmetry with the protons separated as much as possible. The synthesis, structure, and characterization of the materials are reported.



INTRODUCTION

Hydrolysis reactions dramatically influence the chemistry of a metal cation in solution.^{1,2} Actinides are well-known to hydrolyze to form a variety of $\text{An}(\text{OH})_n^{4-n}$ products, the condensation of which can result in the formation of polynuclear compounds, aggregates, and ultimately colloids.^{3–5} Such species are known to impede separation processes^{5,6} and have also been shown to play a significant role in the transport and migration of radionuclides in the environment.^{7–9} Given their importance, research concerning the hydrolysis behavior of An(IV) cations has spanned many decades, yet, even today, the formation, speciation, stability, and reactivity of polynuclear species are not well understood. Our limited knowledge of polymerization reactions precludes a fundamental understanding of metal-ion solution chemistry and speciation and the development of accurate thermodynamic models.

Early investigations into the speciation of dissolved metal ions either ignored or failed to accurately account for the presence of polynuclear complexes. As a result, significant discrepancies in thermodynamic data exist between different studies¹⁰ due, in part, to the use of oversimplified chemical models. Recognizing the importance of oligomeric species in interpreting equilibrium data, Sillen proposed a mathematical analysis to identify and describe the condensation of hydrolyzed species to form polynuclear complexes.^{11,12} Mechanistic understanding has since evolved, and now it is generally accepted that condensation proceeds through either an olation (reaction 1) or oxolation (reaction 2) mechanism resulting in M-OH-M or M-O-M linkages, respectively.^{5,13}



Note that an olation reaction involves only one hydrolyzed ion whereas an oxolation reaction involves two such species and condensation resulting in the formation of a water molecule. The propensity of a metal cation to undergo olation or oxolation is related to the hardness/softness as well as the electronegativity of the metal ion; soft acids favor olation whereas hard acids tend to undergo oxolation.¹³ This distinction can be attributed to the degree to which the metal ion pulls electron density into the M-O(H) bond (i.e., away from the H atom) thus affecting the stability and nucleophilicity of the OH group.

Condensation of tetravalent actinides is generally assumed to occur via an olation mechanism, resulting in –OH bridged polynuclear complexes. For Th(IV), the softest of the tetravalent ions in the Periodic Table, such species are reported to play a critical role in its solution chemistry.^{3,14–22} With an electron configuration of $[\text{Rn}]^0$, Th^{4+} does not exhibit an optical spectrum or *f-f* transitions. Hence the determination of equilibrium constants has historically relied on fitting potentiometric titration data.² Hydrolysis products and polynuclear complexes present in solution are inferred based on chemical intuition coupled with “best fit” models, and the oligomeric species included in the models are rarely supported by structural analysis.

More recently, electrospray ionization mass spectrometry (ESI-MS),^{23,24} laser-induced breakdown detection (LIBD),²⁴ X-ray absorption fine structure (XAFS),^{24–27} large angle X-ray scattering (LAXS),^{28,29} and high energy X-ray scattering (HEXS)^{30,31} have been used to probe Th(IV)-oligomer speciation in aqueous solution. Many polynuclear hydroxide species

Received: July 13, 2011

Published: September 08, 2011

including dimers ($\text{Th}_2(\text{OH})_2^{6+}$; $\text{Th}_2(\text{OH})_3^{5+}$; $\text{Th}_2(\text{OH})_4^{5+}$), tetramers ($\text{Th}_4(\text{OH})_8^{8+}$; $\text{Th}_4(\text{OH})_{12}^{4+}$), pentamers ($\text{Th}_5(\text{OH})_{12}^{8+}$) and hexamers ($\text{Th}_6(\text{OH})_{14}^{10+}$; $\text{Th}_6(\text{OH})_{15}^{9+}$) have been proposed based on inferences from probes of solution speciation, but there is little information available about the solid-state structural chemistry to support or confirm these proposed complexes.^{3,14–17,20–22} Structures containing dimeric,^{30–32} tetrameric,³³ and hexameric²⁶ units as well as hydroxo bridged chains^{34,35} have been isolated.

With the aim of developing a general mechanistic and predictive understanding for the formation of polynuclear metal clusters in solution, we set out to isolate and crystallize stable oligomers that form in aqueous solutions from the condensation of Th hydrolysis products. In hopes of isolating well-defined molecular species, we are examining oligomeric thorium-oxo or thorium-hydroxo bridged complexes that can be isolated and stabilized by monofunctionalized organic acids that permit the isolation of basic polymeric units and the subsequent formation of single crystals suitable for X-ray structural studies. We present here an investigation into the synthesis and structural chemistry of polynuclear Th^{4+} clusters formed at the solubility limit of Th hydrolysis products. After formation, these products are isolated using coordinating carboxylate functionalized ligands. Herein we report on the isolation of hexanuclear Th oxo/hydroxo complexes using three such organic ligands: formate, acetate (OAc), and chloroacetate (CA). Details of the cluster's oxo/hydroxo ligation are supported by electronic structure calculations at the level of density functional theory (DFT) undertaken to provide further insight into the energetics stabilizing the protonation of these hexanuclear Th–O complexes.

EXPERIMENTAL SECTION

Synthesis. Caution! ²³²Th is an alpha emitting radioisotope with a half-life of 1.405×10^{10} years. Standard precautions for handling radioactive materials should be followed when working with the quantities used in the syntheses that follow.

For compounds 1–3, amorphous Th “hydroxide”⁵ was precipitated from a 1 mL solution of 0.5 M $\text{Th}(\text{NO}_3)_4$ in H_2O with NH_4OH . The resulting white precipitate was washed several times with distilled water until the pH of the supernatant was near neutral. Reactions were prepared in either glass tubes or vials. Note: The syntheses described below are those used to obtain crystals suitable for single crystal X-ray diffraction (XRD). Compounds 1–3 can be prepared overnight through evaporation of the mother liquor.

$\text{Th}_6(\text{OH})_4\text{O}_4(\text{H}_2\text{O})_6(\text{HCO}_2)_{12} \cdot n\text{H}_2\text{O}$, **1**. The precipitate was completely dissolved in 2 mL of 1 M formic acid. The solution was then transferred to a watch glass, and evaporation of the solution yielded colorless square plates after several hours to 1 day.

$\text{Th}_6(\text{OH})_4\text{O}_4(\text{H}_2\text{O})_6(\text{OAc})_{12} \cdot n\text{H}_2\text{O}$, **2**. To the precipitate, 5 mL of 0.5 M acetic acid was added. The resulting mixture was centrifuged, and the supernatant was transferred to a glass vial. Evaporation of the solution yielded small colorless blocks after approximately 1 week.

$\text{Th}_6(\text{OH})_4\text{O}_4(\text{H}_2\text{O})_6(\text{CA})_{12} \cdot 4\text{H}_2\text{O}$, **3**. A 5 mL aliquot of 0.5 M CA was added to the precipitate. The slurry was heated at 50 °C. After approximately 1 h the reaction was cooled to room temperature. The resulting mixture was centrifuged and the supernatant was transferred to a watch glass. Colorless plates formed after several hours to days with evaporation of the solution.

X-ray Structure Determination. Reflections were collected at 100 K on a Bruker AXS SMART diffractometer equipped with an APEXII CCD detector using Mo $K\alpha$ radiation. The data were integrated and corrected for absorption using the APEX2 suite of crystallographic software.³⁶ The data of **1** and **2** were also corrected for disordered

Table 1. Crystallographic Data and Structure Refinement for 1–3

	1	2	3
formula	$\text{C}_{12}\text{H}_{28}\text{O}_{38}\text{Th}_6$	$\text{C}_{24}\text{H}_{52}\text{O}_{38}\text{Th}_6$	$\text{C}_{24}\text{H}_{48}\text{Cl}_{12}\text{O}_{42}\text{Th}_6$
MW	2172.58	2340.90	2826.26
temperature (K)	100	100	100
λ (Mo $K\alpha$)	0.71073	0.71073	0.71073
crystal system	orthorhombic	trigonal	triclinic
space group	$Pccn$	$R\bar{3}$	$P\bar{1}$
<i>a</i>	15.649(2)	16.750(2)	11.838(1)
<i>b</i>	18.162(3)	16.750(2)	12.558(1)
<i>c</i>	14.358(2)	19.078(5)	23.747(2)
α	90	90	83.605(1)
β	90	90	88.197(1)
γ	90	120	62.479(1)
<i>V</i>	4080.8(10)	4635.8(13)	3110.6(5)
<i>Z</i>	4	3	2
D_{calc} (g cm^{-3})	3.536	2.515	3.018
μ (mm^{-1})	21.903	14.466	14.904
R_1^a [$I > 2\sigma(I)$]	0.0601	0.0400	0.0516
wR_2^a	0.1591	0.0831	0.1167

$$^a R_1 = \sum ||F_o| - |F_c|| / \sum |F_o|; wR_2 = \{ \sum w(F_o^2 - F_c^2)^2 / \sum w(F_o^2)^2 \}^{1/2}.$$

solvent residing in the voids of the structure using SQUEEZE^{37,38} within PLATON.³⁹ All structures were solved using direct methods and refined using SHELXL-97⁴⁰ in the WinGX software suite.⁴¹ Satisfactory refinements as well as tests for missing symmetry, using PLATON, indicated that no obvious space group changes were needed or suggested. We acknowledge that the structure refinement of **1** is not ideal, and this is attributed to factors that commonly complicate the refinement of polynuclear complexes.⁴² Despite difficulties with the refinement (e.g., problematic thermal parameters for some of the lighter atoms), for the purposes of highlighting the connectivity and composition of the hexanuclear core, descriptions of the refinement and crystal structure of **1** are provided. Crystallographic data for **1–3** are provided in Table 1, and CIF data are available as Supporting Information. Crystallographic data have also been deposited with the Cambridge Crystallographic Database (CCDC) and may be obtained at <http://www.ccdc.cam.ac.uk/> by referencing nos. 821615 (**1**), 821613 (**2**), and 821614 (**3**).

All non-hydrogen atoms were located using difference Fourier maps and were ultimately refined anisotropically. Hydrogen atoms of the μ_3 -hydroxyls on the faces of the clusters were not located during the refinement of compounds **1–3**; however, charge balance requirements for **1–3** and bond valence summation values for **3** (see Supporting Information) suggest protonation of four of the eight oxygen sites on the faces of the hexanuclear core. Hydrogen atoms of the formate groups were placed in calculated positions with distance restraints of 0.93 Å. Hydrogen atoms of the six bound water molecules were not found during the refinement of **1**, but Th–O bond distances for Th1–O5, Th2–O10, and Th3–O16 of 2.648(15), 2.695(14), and 2.664(14) Å, respectively, are consistent with thorium bound water molecules. In **2**, the four μ_3 -OHs may be disordered over the eight μ_3 -O(H) sites on the faces of the cluster, and large anisotropic displacement parameter (ADP) max/min ratios for oxygen atoms O2 and O3 are likely related to the disordered nature of the μ_3 -OH/ μ_3 -O sites. Attempts to locate and split the two sites were unsuccessful. Hydrogen atoms of the bound water molecule (O1) in **2** were found during refinement and refined with distance restraints of 0.80 Å. The hydrogen atoms of the acetate –CH₃ groups were placed in calculated positions, and C–H bond lengths were fixed at 0.96 Å. Hydrogen atoms of the bound and solvent water molecules

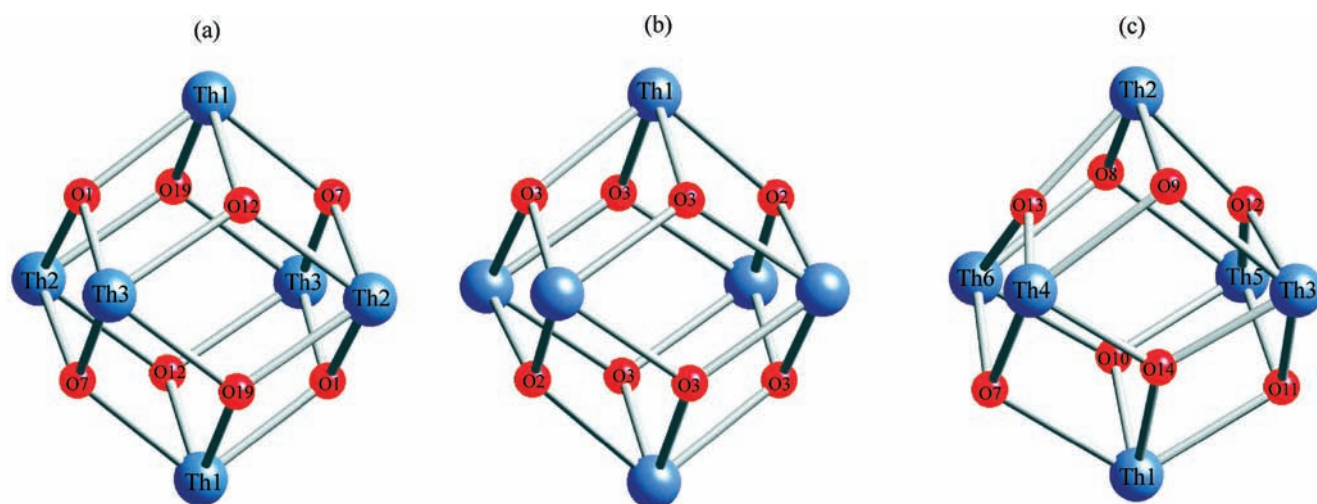


Figure 1. Representation of the $[\text{Th}_6(\text{OH})_4\text{O}_4]^{12+}$ cores in **1** (a), **2** (b), and **3** (c) wherein each Th(IV) center is linked to four additional Th(IV) sites via a combination of μ_3 -hydroxo and μ_3 -oxo bridges. Hydrogen atoms of the μ_3 -hydroxo bridges are not shown. Longer Th–O bonds as well as bond valence summation values suggest protonation of O7–O9 and O11 in **3**. Blue and red spheres represent Th(IV) and oxygen atoms, respectively.

in **3** were not found during refinement; identification of the bound water molecules is evidenced by elongation of the Th–O(H₂) bonds (2.611–2.700 Å) as compared to the average Th–O bond distance (2.51(11) Å). As mentioned previously, hydrogen atoms of the μ_3 -hydroxyl groups on the faces of the clusters were not located during the refinement of **3**. Nonetheless, we discern the μ_3 -OH sites (O7, O8, O9, O11) to be different from the μ_3 -O sites (O10, O12–O14) by inspection of the Th–O bond distances. Average Th–oxygen bond distances for the μ_3 -OH and the μ_3 -O sites were 2.496(13) Å and 2.298(11) Å, respectively. Additionally, bond valence summation values^{43,44} (available as Supporting Information) of ~ 1.2 for the hydroxo oxygen atoms versus ~ 2.0 for the oxo oxygen atoms indicated protonation of O7, O8, O9, and O11. The $-\text{CH}_2$ hydrogen atoms of the monochloroacetate ligand were placed in calculated positions and refined with distance restraints of 0.97 Å. Thermal parameters for disordered solvent water (OW4) and problematic carbon atoms within the disordered part of the structure required constraint of the thermal parameters (EADP) to those of well behaved atoms; this allowed an anisotropic refinement. Disorder within the monochloroacetate units also required the use of restraints; C3–C4A were refined with a bond distance restraint of 1.50 Å while C4(A,B)–Cl2(A,B), and C2A–Cl(A,B) were refined with distance restraints of 1.76 Å.^{45,46} ORTEP illustrations of **1–3** are available in the Supporting Information (SI 1–3).

Powder XRD data were collected for **1–3** using a Scintag X1 diffractometer (Cu K α , 3–40°) and manipulated using Jade.⁴⁷ All peaks in the pattern were indexed using the unit cell obtained from the single-crystal study. Agreement between the calculated and observed patterns confirms that the single crystals used for the structure determination were representative of the bulk sample.

Electronic Structure Calculations. The geometries of **1, 2, 3**, the $\text{Th}_6\text{O}_8^{8+}$ core, the $\text{Th}_6\text{O}_8^{8+}$ core terminated with six O atoms to give $\text{Th}_6\text{O}_8\text{O}_6^{4-}$ and $\text{Th}_6(\text{OH})_4\text{O}_4\text{O}_6$ were optimized using density functional theory (DFT).⁴⁸ The calculations were done with the hybrid B3LYP exchange correlation functional^{49,50} and the local SVWN5 functional.^{51,52} The DZVP basis set⁵³ for H, C, and O (polarized double- ζ on the C and O and double- ζ on the H) and the Stuttgart large core effective core potential and basis set for Th were used for the geometry optimizations.⁵⁴ The f orbitals in the Th basis set were initially excluded because of issues with wave function convergence. Single point energies were calculated with the addition of the innermost two contracted f orbitals to the Th. The calculated structures were all shown to be minima by analysis of the calculated second derivatives. These calculations were done with the Gaussian09 program system.⁵⁵

RESULTS

Synthetic Approach. Hydroxides of the An elements can be obtained by precipitation from aqueous solution by pH adjustment.⁵ Precipitation is preceded by hydrolysis which results in monomeric species that then condense to form polynuclear complexes. In light of this, we explored the formation of oligomeric Th(IV) complexes by precipitating an amorphous product of Th hydrolysis and subsequently saturating an aqueous solution with Th⁴⁺-organic species by addition of organic acids to the precipitate. This approach results in a quantitative yield of the discrete Th(IV) molecular cluster, $\text{Th}_6(\text{OH})_4\text{O}_4(\text{H}_2\text{O})_6(\text{HCOO})_{12} \cdot n\text{H}_2\text{O}$ (**1**), as well as the isolation of two additional hexanuclear clusters, $\text{Th}_6(\text{OH})_4\text{O}_4(\text{H}_2\text{O})_6(\text{CH}_3\text{COO})_{12} \cdot n\text{H}_2\text{O}$ (**2**), and $\text{Th}_6(\text{OH})_4\text{O}_4(\text{H}_2\text{O})_6(\text{ClCH}_2\text{COO})_{12} \cdot 4\text{H}_2\text{O}$ (**3**).

Crystal Structure Description. The structures of **1–3** each consist of a hexanuclear core, $\text{Th}_6\text{O}_4(\text{OH})_4^{12+}$, built from six Th(IV) atoms bridged by four μ_3 -OH and four μ_3 -O groups (Figure 1). Each Th(IV) center is 9-coordinate, bound to four μ_3 -OH/ μ_3 -O oxygen atoms, one bound water molecule and four oxygen atoms from four monodentate R-CO₂[−] (R = -H, -CH₃, or -CH₂Cl) ligands. Overall, the R-CO₂[−] ligands are bridging bidentate and link adjacent Th(IV) centers on the same cluster. As illustrated in Figure 2, the core is a common structural unit in these materials although the core in **3** is slightly distorted compared to that in **1** and **2**. The compounds do differ with respect to crystallographic packing. These subtle differences are attributed to differences in the nature of the anionic organic acids including steric effects, orientations of the R (-H, -CH₃, and -CH₂Cl) group, and hydrogen bonding, as well as the number of solvent water molecules located between the clusters. Selected bond distances for **1–3** are listed in Table 2. Average bond distances for **1–3** are given in Table 3 for comparison with the optimized DFT calculations for the free molecule.

Compound **1** crystallizes in an orthorhombic space group. The structure (Figure 2a) is built from three crystallographically unique Th(IV) metal centers, six unique formate units, four μ_3 -OH/ μ_3 -O sites, and three unique bound water molecules. Each Th(IV) center is bound to four μ_3 -OH/ μ_3 -O oxygen atoms, four carboxylate oxygen atoms from four formate units,

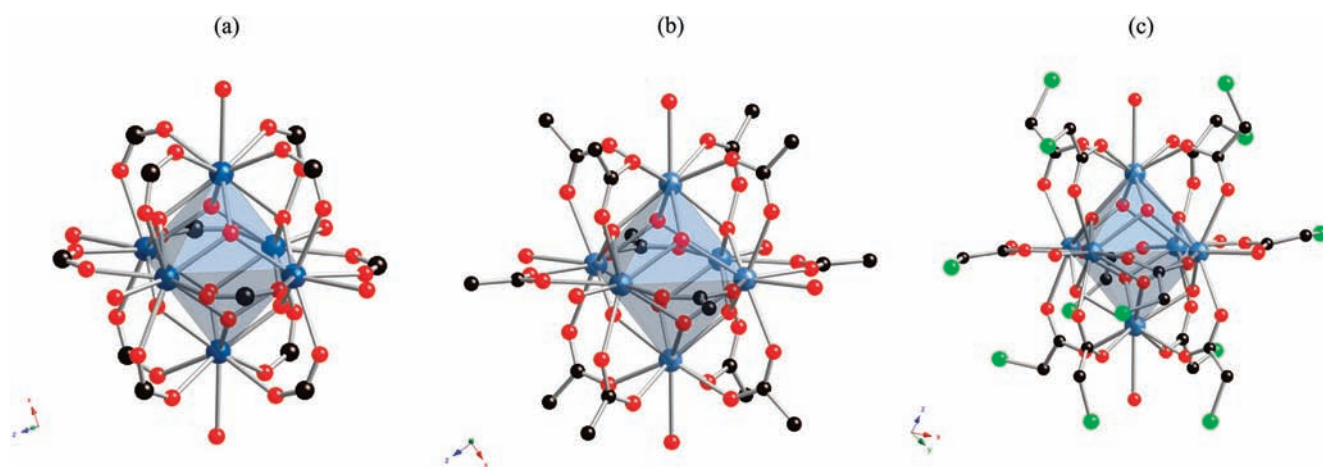


Figure 2. Illustration of the molecular clusters that are built from a hexanuclear $[\text{Th}_6(\text{OH})_4\text{O}_4]^{12+}$ core (blue polyhedra) decorated by (a) 12 formate groups in **1**, (b) 12 acetate ligands in **2**, and 12 monochloroacetate units in **3**. In each compound, the Th(IV) sites are nine-coordinate; each Th^{4+} cation is bound to four oxygen atoms from four acid units, four $\mu_3\text{-OH}/\mu_3\text{-O}$ oxygen atoms and a bound water molecule. Blue spheres are Th(IV) atoms. Red, black, and green spheres represent the oxygen, carbon, and chlorine atoms, respectively, of the R-COO^- ligands ($\text{R} = \text{H}, \text{CH}_3, \text{or } \text{CH}_2\text{Cl}$).

Table 2. Selected Experimental Bond Distances (\AA) for **1–3** from Single Crystal XRD

		1		
Th1–O1	2.379(14)	Th3–O14	2.514(14)	
Th1–O3	2.499(14)	Th3–O16	2.664(13)	
Th1–O5	2.648(15)	C1–O3	1.254(25)	
Th2–O1	2.370(14)	C3–O9	1.258(25)	
Th2–O9	2.501(14)	C–O14	1.223(25)	
Th2–O10	2.695(14)	Th1–Th2	3.912(1)	
Th3–O12	2.380(15)	Th1–Th3	3.939(1)	
		2^a		
Th1–O1	2.621(7)	C1–C2	1.509(14)	
Th1–O2	2.367(5)	C1–O4	1.258(12)	
Th1–O3	2.407(8)	C1–O6 ^{iv}	1.249(11)	
Th1–O4	2.516(7)	Th1–Th1 ⁱ	3.958(1)	
Th1–O5	2.467(7)	Th1–Th1 ⁱⁱⁱ	3.959(1)	
Th1–O6	2.448(7)	Th1–Th1 ^{iv}	3.984(1)	
Th1–O7	2.483(7)			
		3		
Th1–O5	2.700(7)	C19–C20	1.507(14)	
Th1–O7	2.512(7)	C20–Cl10	1.840(12)	
Th1–O10	2.308(7)	Th1–Th3	3.9252(6)	
Th1–O22	2.447(7)	Th1–Th5	3.9170(7)	
Th2–O1	2.699(8)	Th1–Th6	3.9242(6)	
Th2–O8	2.506(7)	Th2–Th4	3.9107(7)	
Th2–O12	2.298(7)	Th2–Th5	3.9129(7)	
Th2–O23	2.463(8)	Th2–Th6	3.9249(6)	
O22–C19	1.268(13)			

^a Symmetry transformations. (2) i = $-y, x-y, z$; ii = $y, -x+y, -z+1$; iii = $-x+y, -x, z$; iv = $x-y, x, -z+1$.

and a bound water molecule at average distances of 2.374(18) \AA , 2.497(17) \AA , and 2.669(24) \AA , respectively. Distances between adjacent Th(IV) atoms range from 3.90 to 3.94 \AA and Th–Th distances between the vertices of the octahedron range from 5.53 to 5.57 \AA .

The structure of **2** is built from one crystallographically unique Th^{4+} metal center, one unique bound H_2O molecule, two unique $\mu_3\text{-O}(\text{H})$ groups, and two unique acetate units. Note that we could not distinguish the $\mu_3\text{-OH}$ from the $\mu_3\text{-O}$ groups in **2** as the hydrogen atoms may be disordered over the oxygen sites, as evidenced by a $\text{Th}-\mu_3\text{-O}(\text{H})$ bond distance that is an average of those reported for $\text{Th}-\mu_3\text{-OH}$ and $\text{Th}-\mu_3\text{-O}$ bonds. This disorder could be due to a “random” distribution of protons on the $\mu_3\text{-OH}$ sites or to disorder of the cationic cluster in the crystal lattice. The latter would result in an average of the $\mu_3\text{-OH}$ and $\mu_3\text{-O}$ sites. The Th–O bond distances are consistent with rotation of the cluster as they are longer than distances reported for Th– $\mu_3\text{-O}$ bonds and shorter than that for a Th– $\mu_3\text{-OH}$ bond. Each Th(IV) site is bound to four bridging $\mu_3\text{-OH}/\mu_3\text{-O}$ oxygen atoms (O2, O3 and their symmetry equivalents), four oxygen atoms from the acetate units (O4–O7) and one oxygen atom from a bound water molecule (O1) at average distances of 2.391(19), 2.479(28), and 2.621(7) \AA , respectively. As shown in Figure 2b, the acetate units are bridging bidentate and link each Th(IV) site to four adjacent Th(IV) centers. Th–Th distances between adjacent atoms and between the vertices of the octahedron (highlighted in blue in Figure 2b) are approximately 3.97 \AA and 5.62 \AA , respectively.

Compound **3** crystallizes in a lower symmetry space group, $P\bar{1}$, and the structure (Figure 2c) is constructed from six crystallographically unique Th(IV) metal centers. Each Th(IV) center is coordinated to two $\mu_3\text{-OH}$ (2.486–2.514 \AA) oxygen atoms, two $\mu_3\text{-O}$ oxygen atoms (2.291–2.315 \AA), four carboxylate oxygen atoms from four chloroacetate units (2.448–2.557 \AA), and a bound water molecule (2.611–2.700 \AA). Distances between adjacent Th(IV) atoms (e.g., Th2–Th3) are 3.91–3.94 \AA . The Th–Th distances between the vertices of the octahedron (e.g., Th1–Th2) range from 5.54 to 5.57 \AA .

ELECTRONIC STRUCTURE RESULTS

As discussed above, the structural studies did not directly locate the H atoms on the Th_6O_8 core during refinement, although charge balance arguments indicate that there are four $\mu_3\text{-OH}$ and four $\mu_3\text{-O}$ groups. Whereas differences in the Th–O bond distances determined for **3** permit the distinction of the

Table 3. Comparison of Average Experimental and Calculated Bond Distances (Å) of Neutral Complexes with Four H⁺ for 1–3

distance	1			2			3		
	expt	B3LYP	SVWN5	expt	B3LYP	SVWN5	expt	B3LYP	SVWN5
Th– μ_3 -O	2.374	2.323	2.287	2.391	2.321	2.287	2.298	2.325	2.290
Th– μ_3 -OH	2.374	2.537	2.493	2.391	2.533	2.488	2.496	2.535	2.486
Th–O–C(R)O	2.497	2.543	2.493	2.479	2.540	2.487	2.501	2.530	2.477
Th–OH ₂	2.669	2.726	2.616	2.621	2.752	2.641	2.656	2.712	2.595
C–O	1.250	1.264	1.263	1.254	1.270	1.269	1.268	1.263	1.263
Th–Th (edge)	3.92	3.981	3.911	3.97	3.977	3.908	3.923	3.987	3.911
Th–Th (vertex)	5.53–5.57	5.631	5.529	5.62	5.625	5.527	5.56	5.638	5.532

Table 4. Optimized Bond Distances for Additional Cluster Structures

distance	4		5		6		7		8	
	B3LYP	SVWN5	B3LYP	SVWN5	B3LYP	SVWN5	B3LYP	SVWN5	B3LYP	SVWN5
Th– μ_3 -O	2.339	2.306	2.401	2.355	2.375	2.329	2.308	2.280	2.306	2.274
Th– μ_3 -OH					2.629	2.559			2.520	2.476
Th–O–C(R)O									2.497	2.442
Th=O			2.033	2.016	1.902	1.891				
C–O							1.262	1.260	1.267	1.264
Th–Th (edge)	3.876	3.826	3.840	3.783	4.005	3.932	3.769	3.721	3.958	3.896
Th–Th (vertex)	5.480	5.411	5.431	5.349	5.664	5.561	5.331	5.262	5.597	5.510

μ_3 -OH and μ_3 -O sites within the core, such is not the case for **1** and **2**, leaving open three possibilities: (i) the proton positions could be “randomly” distributed on the oxygen atoms in the core itself (deemed unlikely), (ii) the protons could be ordered on a Th cluster but the clusters could be randomly oriented in the crystal, or (iii) there could be a dynamic disorder or hopping of the protons among the core oxygen positions. Because details of the proton association with the hexanuclear core may help to provide information relevant to the condensation mechanism responsible for the formation of these clusters, we undertook a computational study of the relative energetics of various isomers of the hexanuclear unit wherein protons occupy different sites.

A number of different hexanuclear Th-cluster structures were optimized as shown in Tables 3 and 4. The structural core, Th₆O₈⁸⁺ (**4**), was first optimized and then six terminal =O atoms were added to the Th atoms to generate a structure with a –4 charge, Th₆O₈O₆^{4–} (**5**). Four H⁺ were then added to structure **5** to form a neutral cluster, Th₆(OH)₄O₄O₆ (**6**) with four μ_3 -OH sites and four μ_3 -O sites. Optimized bond distances for structures **4**–**6** are provided in Table 4. For structure **6**, the four protons were placed on the eight μ_3 -O sites to generate the six possible isomeric structures (**6A**–**6F**) shown in Figure 3. The six terminal =O atoms present in **5** were removed and replaced with 12 bridging formate (HCO₂[–]) groups to give structure **7**, Th₆O₈(HCOO)₁₂^{4–}, that has no μ_3 -OH sites and structure **8** that has four μ_3 -OH sites. Note that the structure of **8** is equivalent to compound **1** (absent, the six H₂O molecules) and its six possible isomers are **8A**–**8F**. Addition of six apical H₂O molecules to structures **4**–**8** to result in nine-coordinate Th(IV) did not affect the structural calculations.

The relative energies of isomers **6A**–**6F** (shown in Figure 3) are given in Table 5. The lowest energy isomer has the four protons arranged in the highest symmetry (pseudo tetrahedral) with two in the upper hemisphere (as far apart as possible) and

two in the lower hemisphere rotated by 90° (**6A**). The structure with the Th terminated with an =O group has the smallest energy differences between the various isomers. Isomer **6B** is closest in energy (8.9 kcal/mol) to the lowest energy structure (**6A**) and has two protons in the upper hemisphere eclipsing two protons in the lower hemisphere. The next highest energy structure (**6F**) has almost the same energy as **6B** (9.0 kcal/mol) and has three protons in the upper hemisphere and one in the lower hemisphere that is located as far as possible from the other protons.

The energy of isomers **1A** to **1F** and **8A** to **8F** were also optimized. The energy differences increase substantially relative to the most stable **A** isomer when the bridging HCO₂[–] groups are used in place of the terminal =O groups; the most stable isomer (**A**) is 13 to 16 kcal/mol more stable than the next most stable isomer (**F**). Isomer **D** is the third most stable isomer for **1** and **8**. The **D** isomer is related to the **F** isomer with three H⁺ in the upper hemisphere and the OH in the lower hemisphere eclipsing the central OH in the upper hemisphere. The effect of substitution of the water molecules on the Th in **1** as compared to **8** is small in terms of the energy differences. The results show that the structures want to separate the protons (excess positive charge) where possible, and the least stable structure has all four protons in the same hemisphere. This suggests that minimizing charge repulsion is important in the proton placement in these structures. However, the presence of the bridging bidentate carboxylate anions can change the stability of the structures relative to the lowest energy structure where the four protons are maximally separated. For **2** and **3**, the **A** isomer and the next lower in energy **F** isomer (as found for **1**) were optimized. Isomer **A** is 12.3 and 8.5 kcal/mol more stable than isomer **F** for **2** and **3**, respectively.

The optimized structural parameters at the B3LYP and SVWN5 levels can be compared to the average experimental values for **1**–**3**. The basic calculated parameters in terms of the

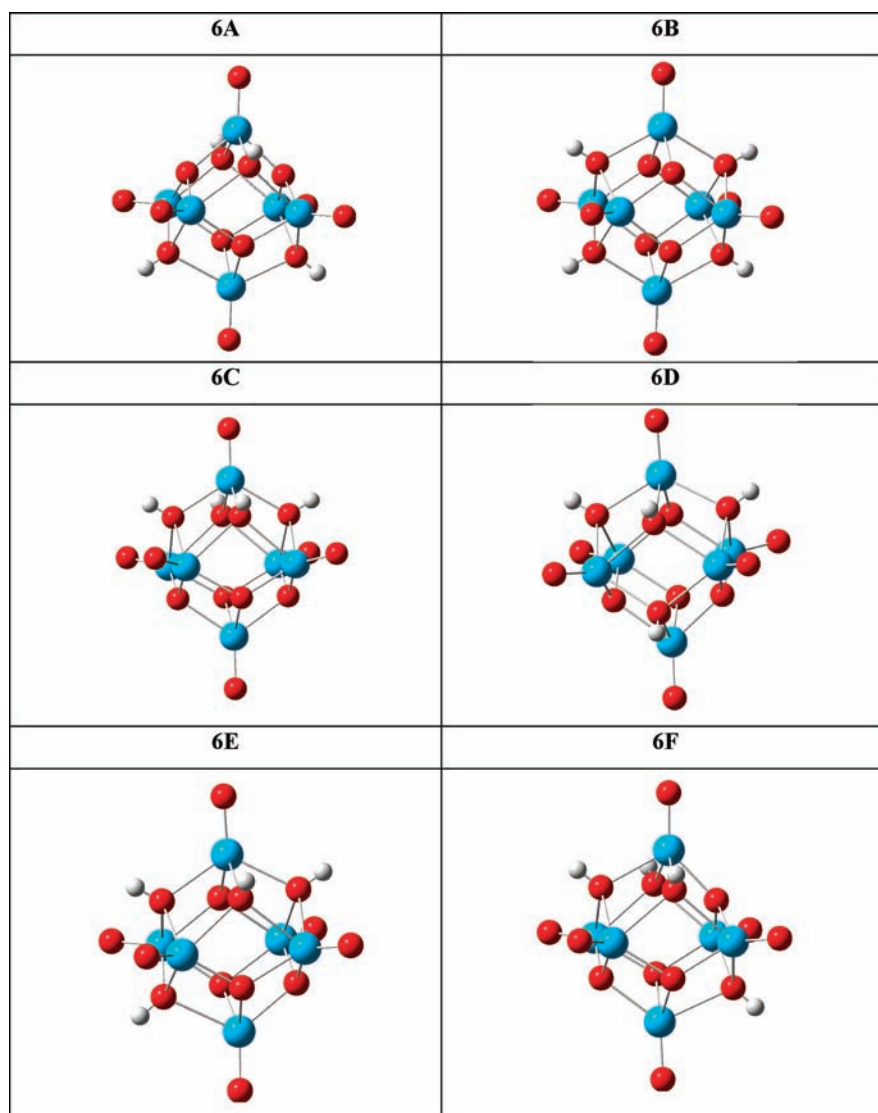


Figure 3. Optimized structures for the six isomers of $6 \text{Th}_6(\text{OH})_4\text{O}_4\text{O}_6$.

Table 5. Calculated Relative Energies in kcal/mol for **1**, **6**, and **8** at the B3LYP/DZVP/Stuttgart Level

isomer	1	6	8
	neutrals		
A	0.0	0.0	0.0
B	17.3	8.9	20.4
C	27.7	22.7	31.5
D	16.6	13.9	19.7
E	21.6	14.4	25.0
F	13.5	9.0	16.1

shape and size of the Th_6O_8 core are in good agreement. The calculated bond distances are a bit larger than those determined experimentally as would be expected with the B3LYP functional and are slightly shorter and in better agreement with experiment for the SVWN5 functional. The calculated $\text{Th}-\mu_3\text{-O}$ bond lengths at both the B3LYP and SVWN5 levels for **1** and **2** are up to 0.1 Å shorter than the average experimental value. The

calculated B3LYP and SVWN5 $\text{Th}-\mu_3\text{-OH}$ bond lengths for **1** and **2** are less than 0.1 Å longer than those observed in the crystal structure. Overall, the calculated $\text{Th}-\mu_3\text{-O}$ bond distances are about 0.2 Å shorter than those calculated for the $\text{Th}-\mu_3\text{-OH}$ bond distances. This compares with an average experimental difference in **3** of 0.198 Å. The $\text{Th}-\text{O}-\text{C}(\text{R})\text{O}$ distances are comparable to the $\text{Th}-\mu_3\text{-OH}$ bond distances within better than 0.02 Å. The longest $\text{Th}-\text{O}$ bond distances are to the H_2O groups solvating the Th consistent with the fact that the H_2O molecules do not bear any formal negative charge as seen in **1–3**.

The presence of six $\text{Th}=\text{O}$ groups to balance the excess positive charge leads to an elongation of the $\text{Th}-\mu_3\text{-O}$ and $\text{Th}-\mu_3\text{-OH}$ bond distances as observed for **5** and **6**, consistent with less positive charge on the Th being available to interact with the negative $\mu_3\text{-O}$ and $\mu_3\text{-OH}$ bridging groups.

DISCUSSION

In contrast to the earlier observations by Johanson,^{5,6} three octahedral-like hexanuclear Th(IV) complexes, $\text{Th}_6(\text{OH})_4\text{O}_4\text{-}(\text{H}_2\text{O})_6(\text{HCOO})_{12}\cdot n\text{H}_2\text{O}$ (**1**), $\text{Th}_6(\text{OH})_4\text{O}_4(\text{H}_2\text{O})_6(\text{CH}_3\text{COO})_{12}\cdot n\text{H}_2\text{O}$ (**2**), and $\text{Th}_6(\text{OH})_4\text{O}_4(\text{H}_2\text{O})_6(\text{ClCH}_2\text{COO})_{12}\cdot 4\text{H}_2\text{O}$ (**3**),

formed through the condensation of hydrolysis products, have been isolated and their structures determined. All three structures are built upon a $\text{Th}_6\text{O}_4(\text{OH})_4^{12+}$ core similar to those previously observed for $\text{Th}(\text{IV})$,^{26,56} as well as other tetravalent metal cations including $\text{Zr}(\text{IV})$,⁵⁷ $\text{Ce}(\text{IV})$,^{58–60} and $\text{U}(\text{IV})$.^{61–66} In fact, such hexanuclear entities appear to be a fundamental building unit in hydrolysis and condensation chemistry, as evidenced by the growing number of structures that contain this moiety.

Such hexanuclear complexes have been synthesized via a number of techniques. With respect to $\text{U}(\text{IV})$ compounds, polynuclear complexes have been obtained from the hydrolysis of $\text{U}(\text{III})$ ⁶⁵ or the reduction of $\text{U}(\text{VI})$ ⁶² in non aqueous systems. Hexanuclear $\text{U}(\text{IV})$ compounds have also been prepared from the disproportionation of $\text{U}(\text{V})$.⁶⁴ For redox inactive metal ions, polynuclear complexes can be prepared from aqueous solutions via evaporation or pH adjustment.^{26,57} Hexanuclear $\text{Ln}(\text{III})$ and $\text{Bi}(\text{III})$ compounds, for example, have been prepared in this manner.^{67–69} The Ln ions adopt a hexanuclear core, yet the structures are different than those reported here as they contain a central $\mu_6\text{-O}$ ligand. In our current study, the formation of oligomeric $\text{Th}(\text{IV})$ complexes was achieved by addition of NH_4OH to an aqueous solution containing 0.5 M thorium nitrate. This resulted in an amorphous Th hydrolysis product that was subsequently dissolved in an aqueous solution containing organic acids, out of which crystals of **1** were obtained in quantitative yield, suggesting that these cationic molecular clusters may be present in the initial amorphous precipitate. The organic acids can serve as a suitable anion for recrystallization.

Compounds **1–3**, together with the hexanuclear Th -formate previously reported by Takao et al.,²⁶ provide structural examples of polynuclear Th^{4+} condensation products that contain both hydroxo and oxo bridges. These examples are chemically different from the $\text{Th}_6(\text{OH})_{14}^{10+}$ and $\text{Th}_6(\text{OH})_{15}^{9+}$ moieties previously suggested as the solution hydrolysis products in thermodynamic speciation scenarios based on olation condensation reactions.^{5,18,19,70} Polynuclear $\text{Th}(\text{IV})$ species and more generally, $\text{An}(\text{IV})$ oligomers, have historically been formulated as $\text{M}_x(\text{OH})_y^{4x-y}$, consistent with an olation mechanism (reaction 1). Until recently, crystal structures supported the formation of polynuclear Th^{4+} complexes with exclusively hydroxide bridges. In an early effort to understand the mechanism of $\text{Th}(\text{IV})$ polymerization to determine whether Th^{4+} formed hydroxo or oxo bridges, Lundgren and Sillen⁷¹ isolated and characterized $\text{Th}(\text{OH})_2\text{CrO}_4\text{H}_2\text{O}$ which consisted of infinite zigzag chains of $[\text{Th}(\text{OH})_2]_n^{2+}$ identical to those observed in the structure of $\text{Th}(\text{OH})_2\text{SO}_4$.³⁴ Johansson later reported the first discrete molecular hydroxo bridged complex, $\text{Th}_2(\text{OH})_2(\text{NO}_3)_6(\text{H}_2\text{O})_6$.³² Since then, a number of structures built from hydroxo bridged dimers have been reported.^{30,72–76} Trimeric and tetrameric complexes solely containing hydroxo bridges have also been isolated.^{33,77} The first hexanuclear Th^{4+} complex was only recently described²⁶ despite the inclusion of such complexes in most chemical models describing the solubility and hydrolysis of $\text{Th}(\text{IV})$. In contrast to the hydroxo bridged species, $\text{Th}_6(\text{OH})_{14}^{10+}$ or $\text{Th}_6(\text{OH})_{15}^{9+}$, commonly accepted to exist in solution⁵ or the μ_3 -oxo hexamer, $[\text{Th}_6\text{O}_8(\text{H}_2\text{O})_n]^{8+}$, more recently proposed,²⁹ all of the hexamers isolated to date contain $\text{Th}(\text{IV})$ centers linked by both μ_3 -hydroxo and μ_3 -oxo groups and are built from the common $[\text{Th}_6(\mu_3\text{-O})_4(\mu_3\text{-OH})_4]^{12+}$ core. This hexanuclear species appears to be a recurrent structural unit that can be isolated

under various synthetic conditions. EXAFS data reported by Takao et al. confirms the presence of the hexamer in solution.²⁶

The DFT calculations predicted that the energetically most favorable oxo/hydroxo arrangement has a tetrahedral arrangement of the OH ions on the octahedral core. This symmetric structure is significantly more stable than the less symmetric isomers, probably because of optimal charge separation of the protons. This energetic result can be used to conclude that it is a disordering of the Th clusters in the molecular structure, and not a static or dynamic disorder of the protons within the cluster itself, that vitiates their direct determination via structural refinement.

Whereas Th^{4+} has tended to form hydroxo, or in the case of the hexamer, hydroxo/oxo bridged polynuclear complexes, other actinides may form different species. For example, to the best of our knowledge, very few hydroxo bridged oligomers have been described for Pu^{4+} .⁷⁸ With respect to higher order polynuclear species, a well-defined $\text{Pu}_{38}\text{O}_{56}$ cluster containing only oxo bridges was recently isolated.⁷⁹ This finding can be used to argue that Pu^{4+} favors an oxolation mechanism for the formation of condensation products. In contrast, exclusively oxo bridged Th^{4+} oligomers have not been reported. Differences in the structural chemistry of Th^{4+} and Pu^{4+} polynuclear species may perhaps be related to the acidity of the metal ion. The charge/size ratio and acidity of the tetravalent actinides follows the general order $\text{Pu}^{4+} > \text{Np}^{4+} > \text{U}^{4+} > \text{Pa}^{4+} > \text{Th}^{4+}$, with $\text{Th}(\text{IV})$ being the softest.⁸⁰ Such subtle differences in acidity likely affect the mechanism by which polynuclear complexes of An^{4+} ions form.

CONCLUSION

Three new hexanuclear $\text{Th}(\text{IV})$ carboxylates have been synthesized under ambient conditions and structurally characterized. The compounds validate our synthesis approach of using pH and temperature to control hydrolysis reactions and then using oxygen donor ligands to capture lower order condensation products. The compounds are built from a $\text{Th}_6(\mu_3\text{-O})_4(\mu_3\text{-OH})_4]^{12+}$ core wherein 9-coordinate Th^{4+} cations are bridged by $\mu_3\text{-O}$ and $\mu_3\text{-OH}$ groups. Electronic structure DFT calculations are used to predict that the OH's arrange on the core in the most symmetric fashion to get optimal charge separation for the protons. The compounds represent examples of Th^{4+} condensation products containing both hydroxo and oxo bridges. Previous examples almost exclusively contained $-\text{OH}$ bridges. Further investigations are needed to fully understand the synthetic role of olation and oxolation reactions within the broader context of polynuclear $\text{An}(\text{IV})$ complex formation.

ASSOCIATED CONTENT

S Supporting Information. ORTEP illustrations of **1–3**. Optimized structures for **1** and **2**, **3** isomers, **6** isomers, and small Th cluster structures. Bond Valence Values for **3**. Total energies in a.u. with the exception of S in cal/mol K at the B3LYP/DZVP+Stuttgart level. Cartesian Coordinates (x , y , z) in Angstroms. This material is available free of charge via the Internet at <http://pubs.acs.org>.

AUTHOR INFORMATION

Corresponding Author

*E-mail: ls@anl.gov.

ACKNOWLEDGMENT

This work was performed in part at the Argonne National Laboratory, operated by UChicagoArgonne LLC for the United States Department of Energy under contract number DE-AC02-06CH11357. The work was supported by a DOE Office of Basic Energy Sciences, Single-Investigator and Small-Group Research Project. D.A.D. is indebted to the Robert Ramsay Endowment of the University of Alabama for partial support.

REFERENCES

- (1) Burgess, J. *Metal Ions in Solution*; Ellis Horwood Limited: Chichester, U.K., 1978.
- (2) Baes, C. F.; Mesmer, R. E. *The hydrolysis of cations*; Wiley: New York, 1976.
- (3) Neck, V.; Kim, J. I. *Radiochim. Acta* **2001**, *89*, 1–16.
- (4) Fanghanel, T.; Neck, V. *Pure Appl. Chem.* **2002**, *74*, 1895–1907.
- (5) Johnson, G. L.; Toth, L. M. *Plutonium(IV) and thorium(IV) hydrous polymer chemistry*; Oak Ridge Natl. Lab.: Oak Ridge, TN, 1978.
- (6) Roberto, J.; de La Rubia, T. D. *Basic Research Needs for Advanced Nuclear Energy Systems, Office of Basic Energy Sciences, U.S. Dept. of Energy, 2006*; <http://iweb.tms.org/NM/NM-0702-2.pdf>.
- (7) Choppin, G. R. *J. Radioanal. Nucl. Chem.* **2007**, *273*, 695–703.
- (8) Novikov, A. P.; Kalmykov, S. N.; Utsunomiya, S.; Ewing, R. C.; Horreard, F.; Merkulov, A.; Clark, S. B.; Tkachev, V. V.; Myasoedov, B. F. *Science* **2006**, *314*, 638–641.
- (9) Kersting, A. B.; Efurud, D. W.; Finnegan, D. L.; Rokop, D. J.; Smith, D. K.; Thompson, J. L. *Nature* **1999**, *397*, 56–59.
- (10) Guillaumont, R.; Fanghanel, T.; Fuger, J.; Grenthe, L.; Neck, V.; Palmer, D. A.; Rand, M. H. *Update on the Chemical Thermodynamics of Uranium, Neptunium, Plutonium, Americium, and Technetium*; Elsevier: Amsterdam, The Netherlands, 2003; Vol. 5, p 970.
- (11) Sillen, L. G. *Acta Chem. Scand.* **1954**, *8*, 318–335.
- (12) Sillen, L. G. *Acta Chem. Scand.* **1954**, *8*, 299–317.
- (13) Henry, M.; Jolivet, J. P.; Livage, J. *Struct. Bonding (Berlin)* **1992**, *77*, 153–206.
- (14) Wickleder, M. S.; Fourest, B.; Dorhout, P. K.; Thorium. In *The Chemistry of the Actinide and Transactinide Elements*, 3rd ed.; Morss, L. R., Edelstein, N. M., Fuger, J., Eds.; Springer: Dordrecht, The Netherlands, 2006; Vol. 1, pp 117–134.
- (15) Hietanen, S. *Acta Chem. Scand.* **1954**, *8*, 1626–1642.
- (16) Hietanen, S.; Sillen, L. G. *Acta Chem. Scand.* **1964**, *18*, 1018–1019.
- (17) Baes, C. F., Jr.; Meyer, N. J.; Roberts, C. E. *Inorg. Chem.* **1965**, *4*, 518–527.
- (18) Hietanen, S.; Sillén, L. G. *Acta Chem. Scand.* **1968**, *22*, 265–280.
- (19) Milić, N. B. *Acta Chem. Scand.* **1971**, *25*, 2487–2498.
- (20) Brown, P. L.; Ellis, J.; Sylva, R. N. *J. Chem. Soc., Dalton Trans.* **1983**, 31–34.
- (21) Ekberg, C.; Albinsson, Y.; Comarmond, M. J.; Brown, P. L. *J. Solution Chem.* **2000**, *29*, 63–86.
- (22) Kraus, K. A.; Holmberg, R. W. *J. Phys. Chem.* **1954**, *58*, 325–330.
- (23) Walther, C.; Fuss, M.; Buchner, S. *Radiochim. Acta* **2008**, *96*, 411–425.
- (24) Rothe, J.; Walther, C.; Brendebach, B.; Buchner, S.; Fuss, M.; Denecke, M. A.; Geckeis, H. *J. Phys.: Conf. Ser.* **2009**, 012188.
- (25) Neck, V.; Muller, R.; Bouby, M.; Altmaier, M.; Rothe, J.; Denecke, M. A.; Kim, J. I. *Radiochim. Acta* **2002**, *90*, 485–494.
- (26) Takao, S.; Takao, K.; Kraus, W.; Emmerling, F.; Scheinost, A. C.; Bernhard, G.; Hennig, C. *Eur. J. Inorg. Chem.* **2009**, 4771–4775.
- (27) Rothe, J.; Denecke, M. A.; Neck, V.; Muller, R.; Kim, J. I. *Inorg. Chem.* **2002**, *41*, 249–258.
- (28) Magini, M.; Cabrini, A.; Scibona, G.; Johansson, G.; Sandstrom, M. *Acta Chem. Scand.* **1976**, *30*, 437–447.
- (29) Torapava, N.; Persson, I.; Eriksson, L.; Lundberg, D. *Inorg. Chem.* **2009**, *48*, 11712–11723.
- (30) Wilson, R. E.; Skanthakumar, S.; Sigmon, G.; Burns, P. C.; Soderholm, L. *Inorg. Chem.* **2007**, *46*, 2368–2372.
- (31) Wilson, R. E.; Skanthakumar, S.; Soderholm, L. *Mater. Res. Soc. Symp. Proc.* **2007**, *986*, 183–188.
- (32) Johansson, G. *Acta Chem. Scand.* **1968**, *22*, 389–398.
- (33) Harrowfield, J. M.; Ogden, M. I.; White, A. H. *J. Chem. Soc., Dalton Trans.* **1991**, 2625–2632.
- (34) Lundgren, G. *Arkiv for Kemi* **1950**, *2*, 535–549.
- (35) Johansson, G. *Svensk Kemisk Tidskrift* **1966**, *78*, 486–489.
- (36) Bruker APEXII Software Suite, v2010.7-0; Bruker AXS: Madison, WI, 2010.
- (37) van der Sluis, P.; Spek, A. L. *Acta Crystallogr., Sect. A* **1990**, *46*, 194–204.
- (38) Using the SQUEEZE routine within the PLATON software package, the total solvent accessible void volume and electron count per cell for **1** were found to be 642.7 Å³ and 167 e⁻, respectively. For **2**, SQUEEZE indicated that the crystals contained 1438.6 Å³ of solvent accessible void and an electron count per cell of 425 e⁻.
- (39) Spek, A. L. *Acta Crystallogr., Sect. A* **1990**, *46*, C34.
- (40) Sheldrick, G. M. *Acta Crystallogr.* **2008**, *A64*, 112–122.
- (41) Farrugia, L. J. *J. Appl. Crystallogr.* **1999**, *32*, 837–838.
- (42) The refinement of polynuclear complexes can be complicated by factors such as strong scattering contrast between the heavy metal atoms and the lighter atoms in the structure as well as disorder of (significant numbers) solvent molecules that are present between clusters. The relatively large R values are thus attributed to these difficulties.
- (43) Brese, N. E.; O'Keefe, M. *Acta Crystallogr.* **1991**, *B47*, 192.
- (44) Brown, I. D. *The Chemical Bond in Inorganic Chemistry: The Bond Valence Model*; Oxford University Press: Oxford, U.K., 2002; p 278.
- (45) Thomas, I. R.; Bruno, I. J.; Cole, J. C.; Macrae, C. F.; Pidcock, E.; Wood, P. A. *J. Appl. Crystallogr.* **2010**, *43*, 362–366.
- (46) Compounds containing chloroacetate units were found using the substructure search function within the WebCSD v1.1.1. The C-C and C-Cl bond distances of 1.50 and 1.76 Å, respectively, used during the refinement of **3** are consistent with the C-C and C-Cl bond distances reported for other compounds containing chloroacetic acid.
- (47) JADE, 6.1; Materials Data, Inc: Livermore, CA, 2002.
- (48) Parr, R. G.; Yang, W. *Density-Functional Theory of Atoms and Molecules*; Oxford University Press: New York, 1989.
- (49) Becke, A. D. *J. Chem. Phys.* **1993**, *98*, 5648–5652.
- (50) Lee, C.; Yang, W.; Parr, R. G. *Phys. Rev. B* **1988**, *37*, 785.
- (51) Slater, J. C. *Phys. Rev.* **1951**, *81*, 385–390.
- (52) Vosko, S. H.; Wilk, L.; Nusair, M. *Can. J. Phys.* **1980**, *58*, 1200–1211.
- (53) Godbout, N.; Salahub, D. R.; Andzelm, J.; Wimmer, E. *Can. J. Chem.* **1992**, *70*, 560–571.
- (54) Kuchle, W.; Dolg, M.; Stoll, H.; Preuss, H. *J. Chem. Phys.* **1994**, *100*, 7535–7542.
- (55) Frisch, M. J.; Trucks, G. W.; Schlegel, H. B.; Scuseria, G. E.; Robb, M. A.; Cheeseman, J. R.; Scalmani, G.; Barone, V.; Mennucci, B.; Petersson, G. A.; Nakatsuji, H.; Caricato, M.; Li, X.; Hratchian, H. P.; Izmaylov, A. F.; Bloino, J.; Zheng, G.; Sonnenberg, J. L.; Hada, M.; Ehara, M.; Toyota, K.; Fukuda, R.; Hasegawa, J.; Ishida, M.; Nakajima, T.; Honda, Y.; Kitao, O.; Nakai, H.; Vreven, T.; J. A. Montgomery, J.; Peralta, J. E.; Ogliaro, F.; Bearpark, M.; Heyd, J. J.; Brothers, E.; Kudin, K. N.; Staroverov, V. N.; Kobayashi, R.; Normand, J.; Raghavachari, K.; Rendell, A.; Burant, J. C.; Iyengar, S. S.; Tomasi, J.; Cossi, M.; Rega, N.; Millam, J. M.; Klene, M.; Knox, J. E.; Cross, J. B.; Bakken, V.; Adamo, C.; Jaramillo, J.; Gomperts, R.; Stratmann, R. E.; Yazyev, O.; Austin, A. J.; Cammi, R.; Pomelli, C.; Ochterski, J. W.; Martin, R. L.; Morokuma, K.; Zakrzewski, V. G.; Voth, G. A.; Salvador, P.; Dannenberg, J. J.; Dapprich, S.; Daniels, A. D.; Farkas, Ö.; Foresman, J. B.; Ortiz, J. V.; Cioslowski, J.; Fox, D. J. *Gaussian 09*, Revision A.2; Gaussian, Inc: Wallingford, CT, 2009.
- (56) Ok, K. M.; O'Hare, D. *Dalton Trans.* **2008**, 5560–5562.
- (57) Pan, L.; Heddy, R.; Li, J.; Zheng, C.; Huang, X.-Y.; Tang, X.; Kilpatrick, L. *Inorg. Chem.* **2008**, *47*, 5537–5539.

- (58) Das, R.; Sarma, R.; Baruah, J. B. *Inorg. Chem. Commun.* **2010**, *13*, 793–795.
- (59) Mereacre, V.; Ako, A. M.; Akhtar, M. N.; Lindemann, A.; Anson, C. E.; Powell, A. K. *Helv. Chim. Acta* **2009**, *92*, 2507–2524.
- (60) Lundgren, G. *Arkiv for Kemi* **1956**, *10*, 183–197.
- (61) Lundgren, G. *Arkiv for Kemi* **1953**, *5*, 349–363.
- (62) Berthet, J.-C.; Thuery, P.; Ephritikhine, M. *Chem. Commun.* **2005**, 3415–3417.
- (63) Mokry, L. M.; Dean, N. S.; Carrano, C. J. *Angew. Chem., Int. Ed.* **1996**, *35*, 1497–1498.
- (64) Mougél, V.; Biswas, B.; Pecaut, J.; Mazzanti, M. *Chem. Commun.* **2010**, *46*, 8648–8650.
- (65) Nocton, G.; Burdet, F.; Pecaut, J.; Mazzanti, M. *Angew. Chem., Int. Ed.* **2007**, *46*, 7574–7578.
- (66) Nocton, G.; Pecaut, J.; Filinchuk, Y.; Mazzanti, M. *Chem. Commun.* **2010**, *46*, 2757–2759.
- (67) Wang, R.; Carducci, M. D.; Zheng, Z. *Inorg. Chem.* **2000**, *39*, 1836–1837.
- (68) Mudring, A. V.; Timofte, T.; Babai, A. *Inorg. Chem.* **2006**, *45*, 5162–5166.
- (69) Lazarini, F. *Acta Crystallogr., Sect. B* **1978**, *35*, 448–450.
- (70) Rand, M.; Fuger, J.; Grenthe, I.; Neck, V.; Rai, D. *Chemical Thermodynamics of Thorium*; Elsevier: Amsterdam, The Netherlands, 2008.
- (71) Lundgren, G.; Sillen, L. G. *Arkiv for Kemi* **1949**, *1*, 277–292.
- (72) Sokolov, M. N.; Gushchin, A. L.; Kovalenko, K. A.; Peresyphkina, E. V.; Virovets, A. V.; Sanchiz, J.; Fedin, V. P. *Inorg. Chem.* **2007**, *46*, 2115–2123.
- (73) Harrowfield, J. M.; Peachey, B. J.; Skelton, B. W.; White, A. H. *Aust. J. Chem.* **1995**, *48*, 1349–1356.
- (74) Rogers, R. D.; Bond, A. H. *Acta Crystallogr., Sect. C* **1992**, *48*, 1199–1201.
- (75) Bino, A.; Chayat, R. *Inorg. Chim. Acta* **1987**, *129*, 273–276.
- (76) Sigmon, G. E.; Burns, P. C. *J. Solid State Chem.* **2010**, *183*, 1604–1608.
- (77) Kadish, K. M.; Liu, Y. H.; Anderson, J. E.; Charpin, P.; Chevrier, G.; Lance, M.; Nierlich, M.; Vigner, D.; Dormond, A.; et al. *J. Am. Chem. Soc.* **1988**, *110*, 6455–6462.
- (78) Wester, D. W. *Inorg. Chem.* **1982**, *21*, 3382–3385.
- (79) Soderholm, L.; Almond, P. M.; Skanthakumar, S.; Wilson, R. E.; Burns, P. C. *Angew. Chem., Int. Ed.* **2008**, *47*, 298–302.
- (80) Shannon, R. *Acta Crystallogr., Sect. A* **1976**, *32*, 751–767.